More Results on Finite Temperature QCD with Wilson Fermions

Szabolcs Borsányi[1], Stephan Dürr[1,2], Zoltán Fodor[1,2,3], Christian Hoelbling[1], Sándor D. Katz[3], Stefan Krieg[1,2], Dániel Nógrádi[3], Kálmán K. Szabó[1], Bálint C. Tóth[1], and Norbert Trombitás[3]

[1] University of Wuppertal, Department of Physics, Wuppertal D-42097, Germany
E-mail: szabo@uni-wuppertal.de

[2] Jülich Supercomputing Centre, Forschungszentrum Jülich, Jülich D-52425, Germany

[3] Eötvös University, Institute for Theoretical Physics, Budapest 1117, Hungary
E-mail: szaboka@general.elte.hu

We investigate $2+1$ flavour QCD thermodynamics using dynamical Wilson fermions in the fixed scale approach. Our previous study at a pion mass of 545 MeV is extended with two additional pion masses, approximately 440 MeV and 280 MeV. We perform simulations using 3 or 4 lattice spacings at each fixed pion mass and measure the renormalised chiral condensate, strange quark number susceptibility and Polyakov loop as a function of the temperature. We observe a decrease in the light chiral pseudo-critical temperature as the pion mass is lowered while the pseudo-critical temperature associated with the strange quark number susceptibility or the Polyakov loop is only mildly sensitive to the pion mass. These findings are in agreement with previous results obtained in the staggered formulation.

1 Introduction

In Refs. 1, 2 we have started a study of $2+1$ flavour QCD thermodynamics using the Wilson fermion formulation. Even though continuum extrapolated results with physical pion masses are already available within the staggered formulation[3–8] the theoretical uncertainty related to the so-called rooting trick necessitates a comprehensive study with a theoretically sound fermion formulation. One example is the Wilson fermion formulation.

In Ref. 2 the pion mass was rather large, around 545 MeV. A careful continuum extrapolation was performed at this fixed pion mass and a comparison was made with similarly continuum extrapolated staggered results and nice agreement was found between the two approaches. In the current work we lower the pion mass and add 440 MeV and 280 MeV to our data set.

The motivation for lowering the pion mass is clearly that we would like to approach the physical pion mass point. But intermediate pion masses, between the physical point and the rather heavy 545 MeV are also important on their own. This is mainly because it was observed in simulations with staggered fermions that the pseudo-critical temperature associated with the light chiral condensate is decreasing as the pion mass is lowered. In order to confirm this phenomenon we have simulated at the intermediate pion masses of 440 MeV and 280 MeV.

The results for these intermediate masses confirm the picture that emerged from the staggered simulations and indeed the light chiral pseudo-critical temperature is decreasing as the pion mass is lowered. On the other hand the pseudo-critical temperature associated

with the confinement-deconfinement transition of the strange quark (given by the strange quark number susceptibility) and the Polyakov loop is only mildly sensitive to the pion masses, again in accordance with the staggered results.

Apart from being theoretically sound another attractive feature of the Wilson formulation using the fixed scale approach is that it complements the staggered formulation using the fixed N_t approach in terms of cut-off effects. More precisely, as a function of temperature the fixed N_t approach has small cut-off effects for high temperature (because of a small bare coupling) and has larger cut-off effects at low temperature (because of a larger bare coupling) while in the fixed scale approach the situation is exactly the opposite: low temperatures correspond to large N_t and hence lead to small cut-off effects while high temperatures correspond to low N_t and hence larger cut-off effects. For further studies of finite temperature QCD using the Wilson formulation see Refs. 9–15.

The organisation of the paper is as follows. In Sec. 2 we summarise the simulation setup, parameters and algorithms that were used. In Sec. 3 the measured observables are given and their renormalisation properties are discussed and in Sec. 4 we present the results of our investigations.

2 Simulation Points and Techniques

The Symanzik tree level improved action[16,17] is used in the gauge sector while in the fermionic sector the clover[18] Wilson action further improved by six steps of stout smearing is adopted[19]. The clover coefficient is set to its tree level value $c_{SW} = 1$ and the stout smearing parameter is chosen at $\varrho = 0.11$. For more details see Ref. 2.

The light quarks u and d are assumed to be degenerate and a $2 + 1$ flavour algorithm is used. The HMC algorithm[20] is adopted for the light quarks and the RHMC algorithm[21] for the strange quark. Various algorithmic improvements are applied for speeding up the simulation: the Sexton-Weingarten multiple time scale integration[22], the Omelyan integration scheme[23] and even-odd preconditioning[24].

Finite temperature simulations of QCD can be carried out in two main approaches (or a mixture of the two). First, in the fixed-N_t approach the bare coupling is used to change the temperature at given temporal lattice extent N_t. Then increasing N_t corresponds to the continuum limit. Second, the fixed scale approach where the temperature is changed by changing N_t at fixed bare coupling β. The continuum limit in this case corresponds to increasing β. While the former is better suited for staggered fermions the latter is more convenient for Wilson fermions and we hence use the latter.

The calculations were performed at the same four gauge couplings as in Ref. 2 $\beta = 3.30$, 3.57, 3.70 and 3.85. The scale was set by $m_\Omega = 1672$ MeV. The temperature at each fixed bare coupling β is varied in discrete steps by varying N_t.

In our past work[2] the pion mass was relatively heavy, around 545 MeV. We will call the simulations at this mass the "heavy" pion mass point.

Two sets of simulations were performed in the current work each corresponding to a fixed m_π/m_Ω and m_K/m_Ω mass ratio. In the first set, which we call "medium" pion mass, the quark masses were tuned to $m_\pi/m_\Omega = 0.264(3)$ and $m_K/m_\Omega = 0.341(2)$. These correspond to about $m_\pi = 440$ MeV and $m_K = 570$ MeV. At this pion mass the simulations were performed at all 4 lattice spacings. Finite volume effects are expected to be small since $m_\pi L > 7$ at each lattice spacing.

β	am_{ud}	am_s	N_s	N_t
3.30	-0.1122	-0.0710	32	6 - 16, 32
3.57	-0.0347	-0.0115	48	6 - 16, 64
3.70	-0.0181	0.0	48	8 - 24, 48
3.85	-0.0100	0.0050	64	8 - 36, 64
β	am_{ud}	am_s	N_s	N_t
3.30	-0.1245	-0.0710	32	6 - 16, 32
3.57	-0.0443	-0.0115	48	8 - 24, 64
3.70	-0.0258	0.0	64	8 - 24, 96

Table 1. Bare parameters for the "medium" pion mass (top) and "light" pion mass (bottom) simulations. The N_t values used for the finite temperature runs and the values used for the zero temperature runs are separated by a comma.

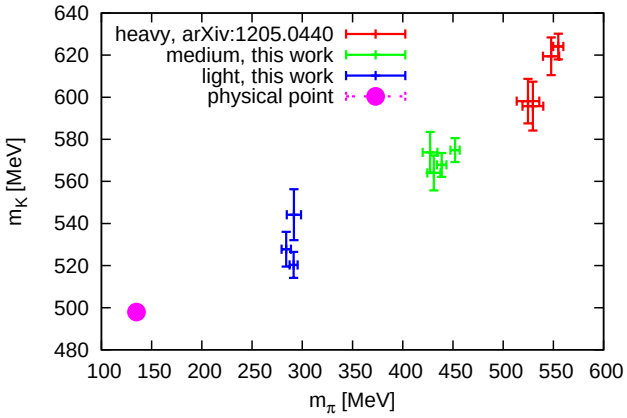

Figure 1. The various pion and kaon masses used in our past and current work. The heaviest pion mass is from our past work[2], the 4 red data points correspond to 4 lattice spacings. For the medium pion mass (this work) also 4 lattice spacings are used, while for the lightest pion mass (this work) we have simulated at 3 lattice spacings. The physical point is also shown for comparison. The scale is set by $m_\Omega = 1672$ MeV.

In the second set, which we call "light" pion mass, the meson masses were tuned to $m_\pi/m_\Omega = 0.171(1)$ and $m_K/m_\Omega = 0.315(3)$, corresponding to about $m_\pi = 280$ MeV and $m_K = 520$ MeV. At these pion masses the simulations were performed at 3 lattice spacings and for the finite volume of the system $m_\pi L > 5.4$ holds.

At each lattice spacing, i.e. fixed β, the mass of the strange quark m_s is fixed at its physical value across all three pion masses "heavy", "medium" and "light" and the physical point is approached by changing m_{ud} only.

A summary of the various pion and kaon masses used in our past and current work is shown on Fig. 1. The bare quark masses, spatial and temporal lattice extents are shown in Tab. 1 while the measured meson, baryon and PCAC masses are shown in Tab. 2. As can be seen m_Ω and hence the lattice spacing depends rather mildly on the light quark masses.

β	m_π/m_Ω	m_K/m_Ω	am_{PCAC}	am_Ω	$a\,[fm]$
3.30	0.262(3)	0.340(3)	0.0248(2)	1.11(1)	0.133(1)
3.57	0.270(3)	0.344(3)	0.01710(5)	0.737(7)	0.088(1)
3.70	0.258(4)	0.337(5)	0.01266(3)	0.578(8)	0.069(1)
3.85	0.256(4)	0.343(6)	0.00890(1)	0.446(7)	0.053(1)
β	m_π/m_Ω	m_K/m_Ω	am_{PCAC}	am_Ω	$a\,[fm]$
3.30	0.174(4)	0.325(7)	0.0084(2)	0.97(2)	0.117(3)
3.57	0.174(2)	0.311(4)	0.00693(4)	0.723(8)	0.087(1)
3.70	0.170(1)	0.316(5)	0.00481(2)	0.560(9)	0.067(1)

Table 2. Spectroscopy and physical scale results from zero temperature simulations, top: "medium" pion mass, bottom: "light" pion mass. The lattice spacings are set by $m_\Omega = 1672$ MeV.

At each finite temperature point around 1000-1500 equilibrated trajectories were generated while around 1000 at zero temperature points.

3 Renormalisation

The temperature dependence of three quantities is determined in the current work, the renormalised light chiral condensate, the strange quark number susceptibility and the renormalised Polyakov loop.

3.1 Chiral Condensate

The bare light chiral condensate requires both additive and multiplicative renormalisation. The details of the full renormalisation procedure is given in Ref. 2 following Refs. 25, 26 and will be summarised below.

Additive renormalisation at $T > 0$ is implemented by the subtraction of $T = 0$ quantities as this difference is free from polynomial divergences. Multiplicative renormalisation is then achieved by the multiplication of the PCAC mass m_{PCAC} and the finite renormalisation constant Z_A. The latter were determined in the chiral limit from 3-flavour simulations in Ref. 2 and can be taken from there directly for each β. Finally the Ward identity establishes a relationship[26] between the chiral condensate and the integrated pion correlator leading to the final expression for the fully renormalised condensate at finite temperature,

$$m_R\langle\bar{\psi}\psi\rangle_R(T) = 2N_f m_{PCAC}^2 Z_A^2 \Delta_{PP}(T)\ , \tag{1}$$

where,

$$\Delta_{PP}(T) = \int d^4x\,\langle P_0(x)P_0(0)\rangle(T) - \int d^4x\,\langle P_0(x)P_0(0)\rangle(T=0)\ , \tag{2}$$

where $P_0(x)$ is the bare pseudo-scalar condensate; for more details see Ref. 2. The final result in Ref. 2 was shown for $m_R\langle\bar{\psi}\psi\rangle_R(T)/m_\pi^4$ since this combination is dimensionless. However when comparing different pion masses as in the current work this normalisation is not convenient because it introduces an artificial pion mass dependence through the 4^{th} power. It turns out that the normalisation $m_R\langle\bar{\psi}\psi\rangle_R(T)/m_\pi^2/m_\Omega^2$ is more suitable as can

be inferred from the GMOR relation as well. All results related to the chiral condensate will be presented with the latter normalisation and also the final result in Ref. 2 will be converted into it for comparison.

3.2 Strange Quark Number Susceptibility

The strange quark number susceptibility χ_s can be made dimensionless by considering χ_s/T^2 and can be improved at tree level by the division of its infinite volume and massless Stefan-Boltzmann limit at each finite N_t. The Stefan-Boltzmann values for each N_t were listed in Ref. 2. The strange quark number susceptibility is sensitive to the confinement-deconfinement temperature of the strange quark and as we will see is only mildly dependent on the pion mass.

3.3 Polyakov Loop

Our renormalisation procedure for the Polyakov loop also follows Ref. 2. The additive divergence of the free energy can be removed by the following renormalisation prescription: a fixed value L_* can be fixed for the renormalised Polyakov loop at a fixed but arbitrary

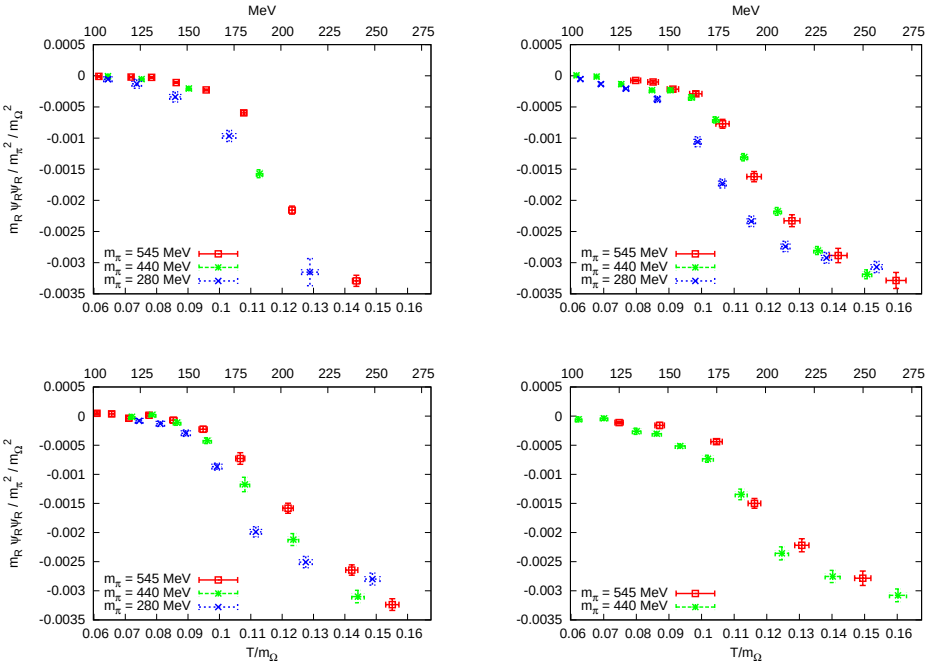

Figure 2. The pion mass dependence of the renormalised chiral condensate at four different lattice spacings. $\beta = 3.30$ (top left), $\beta = 3.57$ (top right), $\beta = 3.70$ (bottom left), $\beta = 3.85$ (bottom right). The data for the "heavy" pion mass (545 MeV) is from Ref. 2. Clearly as the pion mass is decreased the pseudo-critical temperature is also decreasing.

temperature $T_* > T_c$. This prescription leads to the following renormalised Polyakov loop L_R in terms of the bare quantity L_0,

$$L_R(T) = \left(\frac{L_*}{L_0(T_*)} \right)^{\frac{T_*}{T}} L_0(T) \; . \tag{3}$$

We choose $T_* = 0.143 \; m_\Omega$ and $L_* = 1.2$ similarly to Ref. 2 while other choices would simply correspond to other renormalisation schemes.

4 Results

At each fixed pion mass the simulations were performed at several, 3 or 4, bare couplings. These in principle allow for a controlled continuum extrapolation similarly to Ref. 2 but this will be left to a future publication. We however do show one example of the continuum extrapolation which is for the chiral condensate, see below.

The renormalised chiral condensate is shown on Fig. 2 for the four lattice spacings corresponding to the four bare couplings β. On each plot the three pion masses are shown and clearly as the pion mass decreases the pseudo-critical temperature corresponding to the chiral crossover of QCD is seen to decrease as well. This feature is visible at all four lattice

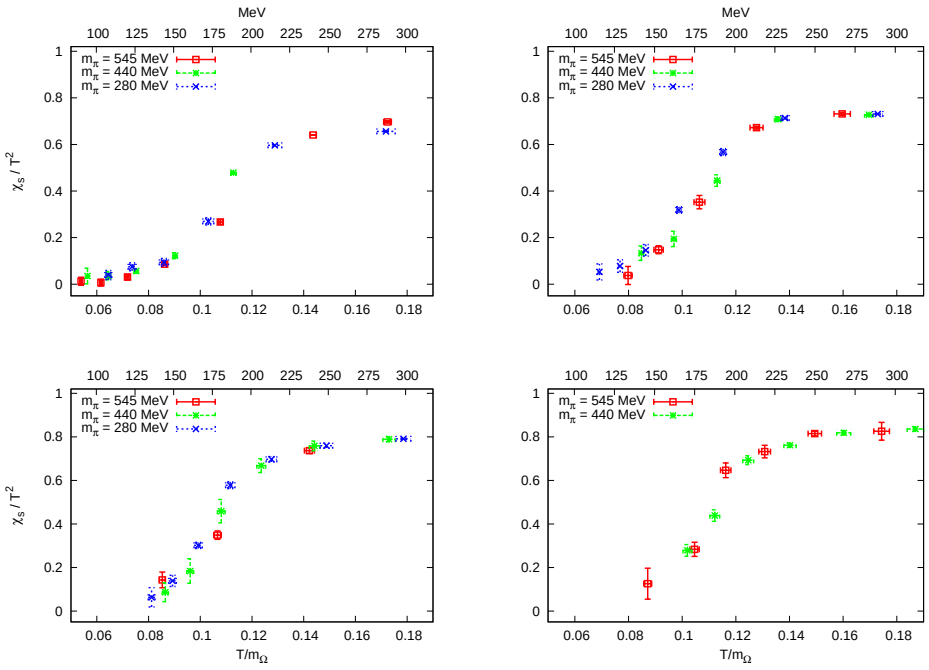

Figure 3. The pion mass dependence of the strange quark number susceptibility at four different lattice spacings. $\beta = 3.30$ (top left), $\beta = 3.57$ (top right), $\beta = 3.70$ (bottom left), $\beta = 3.85$ (bottom right). The data for the "heavy" pion mass (545 MeV) is from Ref. 2. As can be seen the pseudo-critical temperature is only mildly sensitive to the pion mass.

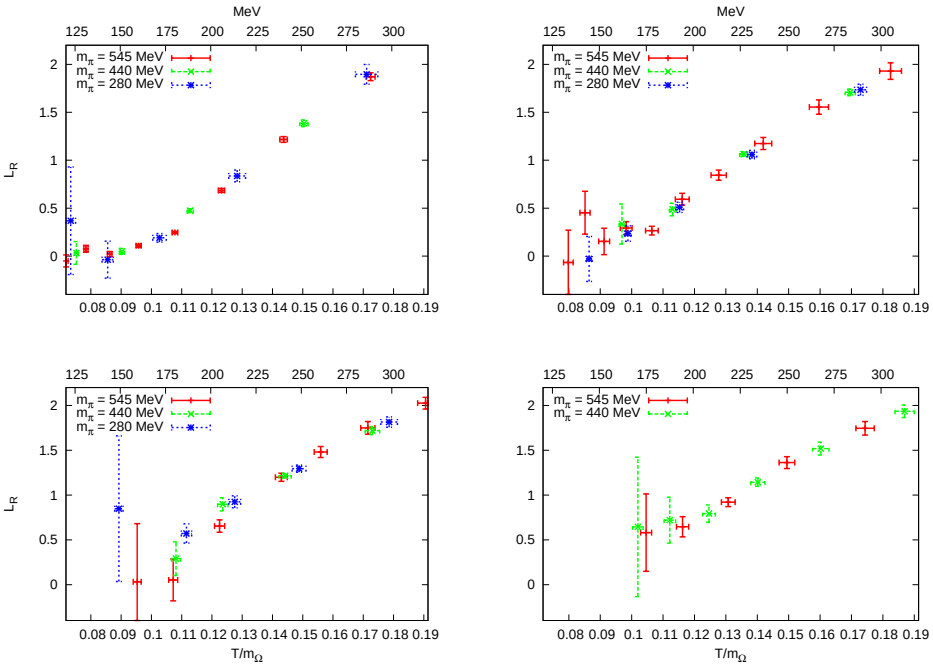

Figure 4. The pion mass dependence of the renormalised Polyakov loop at four different lattice spacings. $\beta = 3.30$ (top left), $\beta = 3.57$ (top right), $\beta = 3.70$ (bottom left), $\beta = 3.85$ (bottom right). The data for the "heavy" pion mass (545 MeV) is from Ref. 2. As can be seen the pseudo-critical temperature is not sensitive to the pion mass at all.

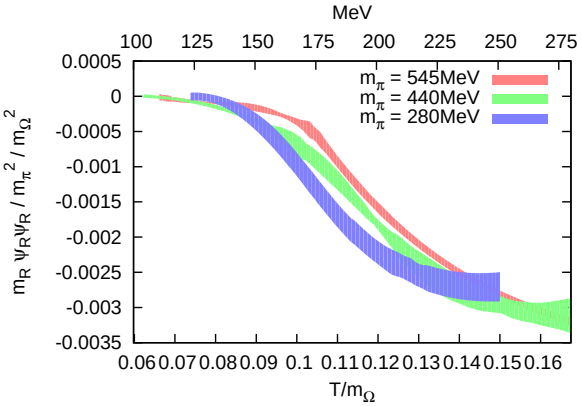

Figure 5. Comparison of the continuum renormalised chiral condensate results for the three pion masses 545 MeV (heavy), 420 MeV (medium) and 280 MeV (light). A downward shift in the pseudo-critical temperature with decreasing pion masses is clearly visible.

spacings we expect the same to hold in the continuum as well. Indeed, as shown on Fig. 5 the continuum results corresponding to the three pion masses also show this behaviour.

The strange quark number susceptibility is shown on Fig. 3 again for all four lattice spacings separately. At each lattice spacing the data for the three pion masses show only mild dependence on the pion mass itself. We have not yet performed a continuum extrapolation of the data but certainly expect that also the continuum result at each pion mass will be only mildly sensitive to the pion mass.

On Fig. 4 our similarly presented data for the Polyakov loop is given. At each of the four lattice spacings the data corresponding to the three pion masses is shown. Just as with the strange quark number susceptibility very little sensitivity to the pion mass is seen. Again, this feature is expected also for the continuum results.

Acknowledgements

Computations were carried out on both GPU clusters[27] at the Universities of Wuppertal and Budapest and also on the Blue Gene/Q computer in Forschungszentrum Jülich. This work was supported by the EU Framework Programme 7 grant (FP7/2007-2013)/ERC No 208740, by the Deutsche Forschungsgemeinschaft grants FO 502/2 and SFB/TRR55 and by the grant OTKA-NF-104034 by OTKA.

References

1. S. Borsanyi, Z. Fodor, C. Hoelbling, S. D. Katz, S. Krieg, *et al.*, *QCD thermodynamics with Wilson fermions*, PoS, **LATTICE2011**, 209, 2011.
2. S. Borsanyi, S. Durr, Z.Fodor, C. Hoelbling, S. D. Katz, *et al.*, *QCD thermodynamics with continuum extrapolated Wilson fermions I*, JHEP, **1208**, 126, 2012.
3. Y. Aoki, G. Endrodi, Z. Fodor, S. D. Katz, and K. K. Szabo, *The Order of the quantum chromodynamics transition predicted by the standard model of particle physics*, Nature, **443**, 675–678, 2006.
4. Y. Aoki, Z. Fodor, S. D. Katz, and K. K. Szabo, *The QCD transition temperature: Results with physical masses in the continuum limit*, Phys. Lett., **B643**, 46–54, 2006.
5. Y. Aoki, S. Borsanyi, S. Durr, Z. Fodor, S. D. Katz, *et al.*, *The QCD transition temperature: results with physical masses in the continuum limit II.*, JHEP, **0906**, 088, 2009.
6. A. Bazavov, T. Bhattacharya, M. Cheng, C. DeTar, H. T. Ding, *et al.*, *The chiral and deconfinement aspects of the QCD transition*, Phys. Rev., **D85**, 054503, 2012.
7. S. Borsanyi *et al.*, *Is there still any T_c mystery in lattice QCD? Results with physical masses in the continuum limit III*, JHEP, **1009**, 073, 2010.
8. S. Borsanyi, Z. Fodor, S. D. Katz, S. Krieg, C. Ratti, *et al.*, *Fluctuations of conserved charges at finite temperature from lattice QCD*, JHEP, **1201**, 138, 2012.
9. T. Umeda, S. Ejiri, S. Aoki, T. Hatsuda, K. Kanaya, *et al.*, *Fixed Scale Approach to Equation of State in Lattice QCD*, Phys. Rev., **D79**, 051501, 2009.
10. S. Ejiri *et al.*, *Equation of State and Heavy-Quark Free Energy at Finite Temperature and Density in Two Flavor Lattice QCD with Wilson Quark Action*, Phys. Rev., **D82**, 014508, 2010.

11. Y. Maezawa *et al.*, *Free energies of heavy quarks in full-QCD lattice simulations with Wilson-type quark action*, Nucl. Phys., **A830**, 247C–250C, 2009.
12. V. G. Bornyakov, R. Horsley, S. M. Morozov, Y. Nakamura, M. I. Polikarpov, *et al.*, *Probing the finite temperature phase transition with $N_f = 2$ nonperturbatively improved Wilson fermions*, Phys. Rev., **D82**, 014504, 2010.
13. T. Umeda *et al.*, *EOS in 2+1 flavor QCD with improved Wilson quarks by the fixed-scale approach*, PoS, **LATTICE2010**, 218, 2010.
14. Y. Maezawa, T. Umeda, S. Aoki, S. Ejiri, T. Hatsuda, *et al.*, *Application of fixed scale approach to static quark free energies in quenched and 2+1 flavor lattice QCD with improved Wilson quark action*, Prog. Theor. Phys., **128**, 955–970, 2012.
15. T. Umeda *et al.*, *Equation of state in 2+1 flavor QCD with improved Wilson quarks by the fixed scale approach*, Phys. Rev., **D85**, 094508, 2012.
16. K. Symanzik, *Continuum Limit and Improved Action in Lattice Theories. 1. Principles and ϕ^4 Theory*, Nucl. Phys., **B226**, 187, 1983.
17. M. Luscher and P. Weisz, *On-Shell Improved Lattice Gauge Theories*, Commun. Math. Phys., **97**, 59, 1985, [Erratum-ibid., **98**, 433, 1985].
18. B. Sheikholeslami and R. Wohlert, *Improved Continuum Limit Lattice Action for QCD with Wilson Fermions*, Nucl. Phys., **B259**, 572, 1985.
19. C. Morningstar and M. J. Peardon, *Analytic smearing of SU(3) link variables in lattice QCD*, Phys. Rev., **D69**, 054501, 2004.
20. S. Duane, A. D. Kennedy, B. J. Pendleton, and D. Roweth, *Hybrid Monte Carlo*, Phys. Lett., **B195**, 216–222, 1987.
21. M. A. Clark and A. D. Kennedy, *Accelerating dynamical fermion computations using the rational hybrid Monte Carlo (RHMC) algorithm with multiple pseudofermion fields*, Phys. Rev. Lett., **98**, 051601, 2007.
22. J. C. Sexton and D. H. Weingarten, *Hamiltonian evolution for the hybrid Monte Carlo algorithm*, Nucl. Phys., **B380**, 665–678, 1992.
23. T. Takaishi and P. de Forcrand, *Testing and tuning new symplectic integrators for hybrid Monte Carlo algorithm in lattice QCD*, Phys. Rev., **E73**, 036706, 2006.
24. T. A. DeGrand, *A Conditioning Technique for Matrix Inversion for Wilson Fermions*, Comput. Phys. Commun., **52**, 161–164, 1988.
25. M. Bochicchio, L. Maiani, G. Martinelli, G. C. Rossi, and M. Testa, *Chiral Symmetry on the Lattice with Wilson Fermions*, Nucl. Phys., **B262**, 331, 1985.
26. L. Giusti, F. Rapuano, M. Talevi, and A. Vladikas, *The QCD chiral condensate from the lattice*, Nucl. Phys., **B538**, 249–277, 1999.
27. G. I. Egri, Z. Fodor, C. Hoelbling, S. D. Katz, D. Nogradi, *et al.*, *Lattice QCD as a video game*, Comput. Phys. Commun., **177**, 631–639, 2007.